Electron Density Modulations in Columnar Banana Phases

Ewa Gorecka,*,† Nataša Vaupotič,‡,§ and Damian Pociecha†

Department of Chemistry, Warsaw University, Al. Zwirki i Wigury 101, 02-089 Warsaw, Poland, Department of Physics, Faculty of Natural Sciences and Mathematics, University of Maribor, Koroška 160, 2000 Maribor, Slovenia, and Jozef Stefan Institute, Jamova 39, 1000 Ljubljana, Slovenia

Received October 26, 2006. Revised Manuscript Received March 14, 2007

The structure of columnar phases formed by bent-core mesogens is analyzed. The combination of the X-ray diffraction intensity data and the model predictions for the form factor phases allows for the construction of the electron density maps for these phases. Within the model, the smectic layer fragments are approximated by parallelograms placed in a body-centered crystallographic unit cell, the parallelogram size and orientation with respect to the unit cell sides being the free parameters. Obtained maps show that in the tilted columnar phase, the neighboring molecular blocks with opposite electric polarity are connected either through the walls or continuously by the less-ordered layer fragments. The type of connection between the blocks seems to be determined by the size of the crystallographic unit cell.

Compared to the classical rodlike systems, bent-core molecules display a surprisingly high variety of liquid crystalline (LC) phases with two-dimensional (2D) electron density modulations.[1] There are two major types of 2D modulated structures, undulated lamellar and columnar. Polarization splay leads to undulation of the smectic layers;[2,3] the resulting structure is called the polarization modulated and layer undulated (PM/LU) phase (also called B_7 phase). It might also lead to the layer breakage and formation of layer fragments, which are arranged into stacks forming columnar structures. If molecules are not tilted with respect to the layer normal, these fragments form a rectangular lattice with the neighboring columns being antiferroelectric. In each block, electric polarization vector is oriented in the direction perpendicular to the 2D lattice (B_{1Rev} phase[4]). When the molecules tilt with respect to the layer normal the unit cell is in general oblique ($B_{1RevTilted}$ phase[4,5]). A few structural models have been proposed to describe the molecular organization in the columnar phases. The simplest model[4] with uniform orientation of the molecules inside the layer fragment could not explain the X-ray data in some materials with the oblique $B_{1RevTilted}$ phase, so more elaborate models with modulated orientation[6] or position[7] of the molecules in the layer fragments were proposed.

The basic arrangement of the layer fragments, i.e., the crystallographic unit cell, is easily determined from the position of the X-ray signals. However, the determination of the electron density distribution within the cell is a rather difficult problem. To obtain position and orientation of the molecular blocks (motifs) in the unit cell or the undulated (ripple) patterns, we have to know both the amplitude and the phase of form factors (i.e., Fourier transform coefficients of the electron density distribution that, in general, are complex numbers) for all the measured X-ray signals. The information about the form factor amplitudes can be acquired from the X-ray peak intensities while there is no universal method to determine the form factor phases, because the standard procedures[8] used for solid crystals are not applicable in the soft matter X-ray diffraction. For high-symmetry structures, commonly considered for the 2D modulated banana phases, the form factor phases take the value 0 or π, and thus there is a possibility of deducing the electron density profile by generating the maps for all possible combinations of the form factor signs (2^n possibilities, where n is the number of signals)[7] and choosing the most "physical" map by intuition. This is not an easy task, even for LC phases where usually only few signals are observed, because, e.g., six signals require checking of 64 maps.

Instead of testing all the possible sign combinations, a simple model for the electron density distribution is constructed. The possible signs of the form factors are obtained from the model and then used in combination with the experimental X-ray signal intensities. If the resulting experimental map reproduces the initial model, one can safely assume that the model is close to reality.

In the present study, we reanalyze the X-ray diffraction data obtained for compound **1** (Figure 1) in which the B_{1Rev}

* Corresponding author. E-mail: gorecka@chem.uw.edu.pl.
† Warsaw University.
‡ University of Maribor.
§ Jozef Stefan Institute.

(1) See for example reviews by Reddy, R. A.; Tschierske, C. *J. Mater. Chem.* **2006**, *16*, 907. Takezoe, H.; Takanishi, Y. *Jpn. J. Appl. Phys.* **2006**, *45*, 597.
(2) Coleman, D. A.; Fernsler, J.; Chattham, N.; Nakata, M.; Takanishi, Y.; Korblova, E.; Link, D. R.; Shao, R. F.; Jang, W. G.; Maclennan, J. E.; Mondainn-Mova, O.; Boyer, C.; Weissflog, W.; Pelzl, G.; Chien, L. C.; Zasadzinski, J.; Watanabe, J.; Walba, D. M.; Takezoe, H.; Clark, N. A. *Science* **2003**, *301*, 1204.
(3) Vaupotič, N.; Čopič, M. *Phys. Rev. E* **2005**, *72*, 031701. Vaupotič, N. *Ferroelectrics* **2006**, *344*, 151.
(4) Szydlowska, J.; Mieczkowski, J.; Matraszek, J.; Bruce, D. W.; Gorecka, E.; Pociecha, D.; Guillon, D. *Phys. Rev. E* **2003**, *67*, 031702.
(5) Mieczkowski, J.; Gomola, K.; Koseska, J.; Pociecha, D.; Szydlowska, J.; Gorecka, E. *J. Mater. Chem.* **2003**, *13*, 2132.
(6) Folcia, C. L.; Etxebarria, J.; Ortega, J.; Ros.; M. B. *Phys. Rev. E* **2005**, *72*, 041709.
(7) Folcia, C. L.; Alonso, I.; Ortega, J.; Etxebarria, J.; Pintre, I.; Ros, M. B. *Chem. Mater.* **2006**, *18*, 4617.

10.1021/cm0625575 CCC: $37.00
Published on Web 05/02/2007

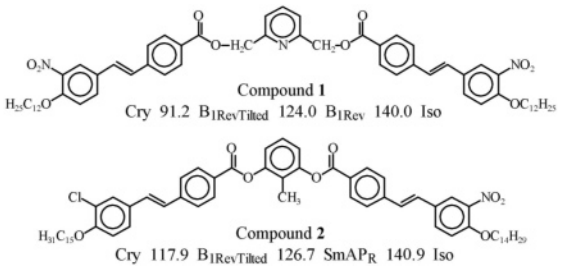

Figure 1. Molecular structure and the phase sequence for the compounds **1** and **2**. In compound **1**, two columnar phases $B1_{RevTilted}$ and B_{1Rev} are detected betweenthe crystal (Cry) and isotropic (Iso) phases. In compound **2**, the columnar phase is detected below the lamellar nontilted polar phase ($SmAP_R$).

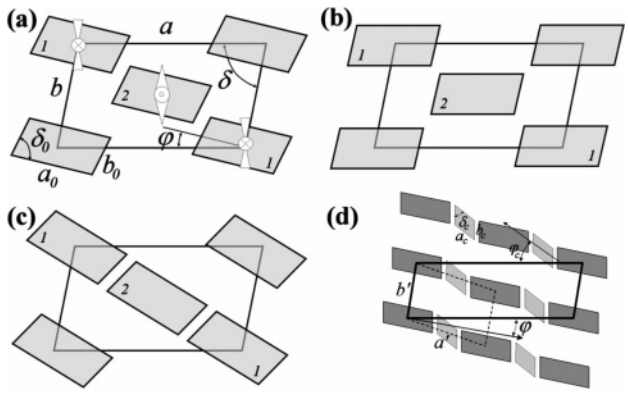

Figure 2. (a) Schematic drawing of the 2D modulated banana phase structure with the parameters used in the model. The orientation of the bent-shaped molecules in the blocks is presented. The blocks labeled 1 and 2 differ in the molecular tips (and thus polarization) direction. (b) Ideal $B_{1RevTilted}$ phase structure, where the blocks with the opposite polarization, 1 and 2, are relatively shifted by $b/2$. (c) Nearly lamellar structure obtained by rotation of the blocks into the direction of the cell diagonal. (d) Ripple layer structure; additional parameters used in the model are indicated. The possible primitive crystallographic unit cell (with unit vectors a' and b') is drawn by dotted line.

(rectangular lattice) and $B_{1RevTilted}$ (oblique lattice) phases were observed,[4] and results are compared with those obtained for a chemically similar compound **2**,[5] showing a 2D modulated phase below a lamellar one.

The powder diffraction data were analyzed, as monodomain samples are usually impossible to grow for bent-shaped mesogens. Samples were prepared in Lindemann capillaries, CuK_α radiation was used, and the patterns were registered with a 2D position-sensitive detector (Bruker Nanostar system). The signal intensities were obtained through integration of the pattern over the azimuthal angle. The main Bragg reflections used in electron density map construction were in the range of 2°, thus the Lorentz-polarization corrections to the intensity were ignored[9] and only the signal multiplicity factor is taken into account for the intensity of the peaks.

For the indexing of the maxima of the diffraction, a 2D, body-centered crystallographic unit cell was chosen (Figure 2). This seems a more appropriate choice than the smallest, primitive cell, because the primitive cell might not reproduce the full symmetry of the antiferroelectric structure.[4,6] The unit cell is rectangular or oblique for B_{1Rev} and $B_{1RevTilted}$ phases, respectively. The crystallographic unit cell parameters obtained from the X-ray studies are given in Table 1. The X-ray intensities for the B_{1Rev} phase of material 1 are given in Table 2, and for the $B_{1RevTilted}$ phase of materials 1 and 2, they are given in Table 3.

In theoretical considerations, a model with a parallelogram as a structural motif of the crystallographic unit cell is used. The motif (block) size and orientation with respect to the unit-cell sides are free parameters in the model (Figure 2). Keeping the same crystallographic unit cell and rotating the blocks allows for an easy prediction of the X-ray diffraction pattern for a variety of structures. It should be noticed that the rotation of the blocks changes the degree of "lamellarization" in the system. If the blocks are oriented along the diagonal of the unit cell, a lamellar structure is obtained (Figure 2c), which must involve polarization deformation regions between blocks of opposite polarization direction. For the blocks oriented along the side of the unit cell (Figure

Table 1. Crystallographic Unit-Cell Parameters Obtained from X-ray Measurements in Compounds 1 and 2

compd/phase	a (nm)	b (nm)	δ (deg)
1/B_{1Rev}	15.4	5.35	90
1/$B_{1RevTilted}$	12.9	5.12	79.3
2/$B_{1RevTilted}$	23.3	5.21	83.1

Table 2. Experimental (I_{exp}) and Theoretical (I_{th}) Peak Intensities and Form Factor Phases (ϕ) for Orthogonal B_{1Rev} Phase in Compound 1; Model Parameters: $\varphi = 0$, $a_0 = 0.30a$, $b_0 = 0.30b$, $\delta_o = 90°$

(h,k)	I_{exp}	I_{th}	ϕ
(2,0) (−2,0)	27	26	0
(1,1) (−1,−1)	100	100	0
(1,−1) (−1,1)			
(3,1) (−3,−1)	4	4	0
(3,−1) (−3,1)			
(0,2) (0,−2)	11	26	0
(2,2) (−2,−2)	23	16	0
(2,−2) (−2,2)			
(3,3) (−3,−3)	1	0.4	0
(3,−3) (−3,3)			

Table 3. Experimental (I_{exp}) and Theoretical (I_{th}) Peak Intensities and Form Factor Phases (ϕ) for $B_{1RevTilted}$ Phase in Compounds 1 and 2[a]

	compound **1**			compound **2**			
(h,k)	I_{exp1}	I_{th1}	ϕ_1	I_{exp2}	I_{th2}	I_{th2}^A	ϕ_2
(2,0) (−2,0)	16	10	0	3	4	3	0
(1,1) (−1,−1)	100	100	0	100	100	100	0
(1,−1) (−1,1)	25	33	0	13	27	18	0
(3,1) (−3,−1)	4.8	0.02	π	2.7	2	2	π
(−3,1) (3,−1)	0.5	4	π	0.8	4	0.7	π
(0,2) (0,−2)	25	28	0	2.3	3	2	0
(2,2) (−2,−2)		24	0		3	3	0
(2,−2) (−2,2)	4.0	0.4	π				
(3,3) (−3,−3)	1.0	1	0				
(4,0) (−4,0)	2.0	5	π	2	4	1	π
(4,4) (4,−4)	2.0	0.01	π				

[a] The model parameters (see Figure 2a) were $a_0 = 0.38a$, $b_0 = 0.30b$, $\delta_0 = 100°$, and $\varphi = 10°$ for compound **1** and $a_0 = 0.43a$, $b_0 = 0.43b$, $\delta_0 = 100°$, and $\varphi = 5°$ for compound **2**. The structure of compound **2** was also analyzed (I_{th2}^A) with the model, assuming anticlinic block arrangement (see Figure 2d) with parameters $a_0 = 0.38a$, $b_0 = 0.43b$, $\delta_0 = 100°$, and $\varphi = 5°$ for the main blocks and $a_c = 0.08a$, $b_c = 0.40b$, $\delta_c = 130°$, $\varphi_c = 40°$, and $\rho = 0.8$ for the "connecting" blocks. In both materials, the signals (02) and (22) could not be resolved in the experiment; their intensity is summed up.

(8) Van Meerssche, M.; Feneau-Dupont, J. *Introduction a la Cristallographie et a la Chimie Struturale*, 2nd ed.; Peeters: Paris, 1976.
(9) Als-Nielsen, J.; McMorrow, D. *Elements of Modern X-ray Studies*; John Wiley & Sons: Chichester, UK, 2001.

2b) the columnar structure with a "half-layer" shift between the columns of opposite polarization is achieved (ideal B_{1Rev} phase).

For the considered crystallographic unit cell with a base at the position $\bar{r}_b = (\bar{a} + \bar{b})/2$ the form factors are $F(h,k) = f_B(1 + \exp\{i\bar{q}\cdot\bar{r}_b\}) = f_B(1 + \exp\{i\pi(h + k)\})$, where h and k are integer numbers.[10] The coefficient f_B is the Fourier transform of the motif

$$f_B = \int\int_S \exp\{i\bar{q}\cdot\bar{r}\}dxdz = S\int_{-1/2}^{1/2} d\beta \exp\{i\bar{q}\cdot\bar{r}\} \quad (1)$$

where S is the area of the block. The wave vector $\bar{q}$ in the reciprocal space is

$$\bar{q} = h\bar{q}_a + k\bar{q}_b = \left\{\frac{2h\pi}{a}, -\frac{2h\pi}{a\tan\delta} + \frac{2k\pi}{b\sin\delta}\right\}$$

The vector $\bar{r} = \alpha\bar{a}_0 + \beta\vec{b}_0$ points inside the block if parameters α and β run from $-1/2$ to $1/2$. To have f_B as a real number, the origin of the coordinate system is set in the center of the block. The integration over the whole block gives

$$f_B = \frac{a^2b^2\sin^2\delta \sin\left[\frac{a_0\pi C_1}{ab\sin\delta}\right]\sin\left[\frac{b_0\pi C_2}{ab\sin\delta}\right]}{\pi^2 C_1 C_2} \quad (2)$$

where:

$$C_1 = bh\sin(\delta + \varphi) - ak\sin\varphi \quad \text{and}$$
$$C_2 = bh\sin(\delta - \delta_0 + \varphi) + ak\sin(\delta_0 - \varphi)$$

with the angles δ, δ_0, and φ and dimensions a, b, a_0, b_0 being defined in Figure 2. The sign of f_B defines the 0 or π phase of the form factor.

A model in which the electron density at the motif edges is lowered was also tested; however, this complication did not considerably improve the agreement between the theory and experiment. Because the model serves only to obtain qualitative agreement in the theoretical and experimental electron density maps, only the uniform density for the blocks was considered.

The unit-cell parameters (a, b, and δ) are taken from the analysis of the X-ray peak positions. The block parameters (dimensions a_0, b_0, and angle δ_0) and the angle of the block rotation (φ) were adjusted to obtain relative intensities of the strongest diffraction signals in a qualitative agreement with the experiment. The electron density maps, $\rho_{exp}(x,z)$, were produced by taking experimentally obtained peak intensities $I_{exp}(h,k)$ in combination with form factor phases $\phi(h,k)$ calculated from the model as $\rho_{exp}(x,z) = \sum_{h,k}\sqrt{I_{exp}(h,k)}\cos(q_x x + q_z z + \phi(h,k))$. For comparison, the theoretical electron density maps, $\rho_{th}(x,z)$, were also created using the calculated form factors $F(h,k)$: $\rho_{th}(x,z) = \sum_{h,k}F(h,k)\cos(q_x x + q_z z)$, where only the (h,k) signals that are experimentally available were summed up.

The proposed model, in which a body centered crystallographic unit cell is used, can also be adopted to account for the ripple (undulated) phase structure by assuming the anticlinic block arrangement. In this case, there are four blocks in the unit cell, as shown in Figure 2d, two main blocks are placed at positions (0, 0) and (a/2, b/2) and two connecting blocks at positions (a/4, 3b/4) and (3a/4, b/4) or at positions (a/4, b/4) and (3a/4, 3b/4), depending on whether the connection is along the short or the long diagonal, respectively. The resulting form factors are

$$F(h,k) = (f_{B1} + \rho f_{B2}\exp\{i(\pm h + k)\pi/2\})(1 + \exp\{i(h + k)\pi\})$$

where "+" is for the connection along the long diagonal and "−" for the connection along the short diagonal. The Fourier transforms of the main and the connecting blocks (f_{B1} and f_{B2}) are calculated from eq 1, taking into account that the motif parameters are in general different for the main and the connecting blocks. The parameter ρ is introduced because the electron density in the connecting block might be different from the density in the main block. Alternatively, the X-ray diffraction pattern of the anticlinic block structure can also be analyzed assuming a face-centered crystallographic unit cell (base placed at (a'/2, 0) position, see Figure 2d), for which form factors are $F(h,k) = f_{B1} + \rho f_{B2}\exp\{ih\pi\}$. In this model, the deformation of an ideally flat layer structure into ripples obviously decreases the intensity of the (01) signal (that corresponds to the signal (11) in the centered cell) in favor of the (11) and (−11) signals (corresponding to (31) and (−11) signals in the centered cell). For a symmetric anticlinic ripple phase the model predicts that the form factors of the signals (11) and (−11) have the same amplitudes but opposite signs. The possible asymmetry in the ripple structure (the difference in the inclination angle, size, shape, or electron density of the blocks) is reflected in different amplitudes of the form factors, thus different intensities, of the signals (11) and (−11).

In the B_{1Rev} phase the unit cell is rectangular ($\delta = 90°$) made of rectangular blocks ($\delta_0 = 90°$). We assume that the blocks are not rotated with respect to the unit-cell side ($\varphi = 0$). Under these conditions the Fourier transform of the motif (eq 2) reduces to

$$f_B = \frac{ab\sin\left[\frac{a_0\pi h}{a}\right]\sin\left[\frac{b_0\pi k}{b}\right]}{\pi^2 hk}$$

If for positive h and k the conditions $a_0/a < 1/h$ and $b_0/b < 1/k$ are satisfied, then f_B is always positive. Because a_0/a and b_0/b should both be less than 1/2, only the form factors f_B corresponding to signals (31) and (33) might be negative and thus have phase π. The f_B for signal (31) is negative if $a_0/a > 1/3$ and for signal (33) f_B is negative if either $a_0/a > 1/3$ or $b_0/b > 1/3$ (but not both). This reduces the problem of finding the correct form factor phases to only four possible configurations. For material **1** in the orthogonal B_{1Rev} phase, the satisfactory agreement between the model and experimental maps and the relative peak intensities was obtained if dimensions of the motif are $a_0 = 0.30a$, $b_0 = 0.30b$, $\delta_0 = 90°$, which implies that all the form factor

(10) Chaikin, P. M.; Lubensky T. C. *Principles of Condensed Matter Physics*; Cambridge University Press: Cambridge, UK, 1995.

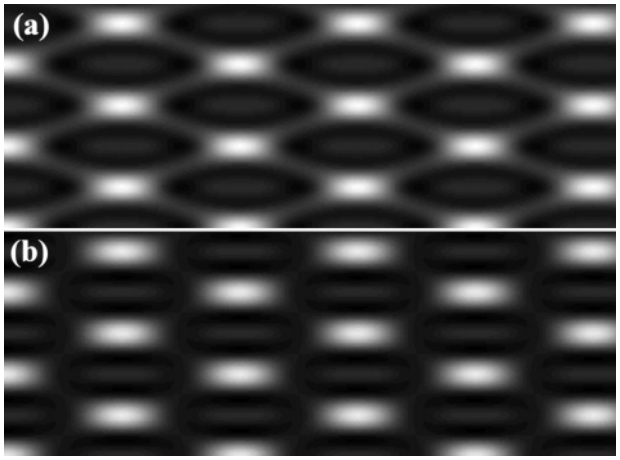

Figure 3. Experimental (a) and theoretical (b) electron density maps for the B_{1Rev} phase of compound **1**. The brightness in the pattern is proportional to the electron density. In both maps, the low-density regions are not completely uniform because of a lack of higher harmonics ($h,k > 3$) that are of too low intensity to be observed in the standard X-ray experiment.

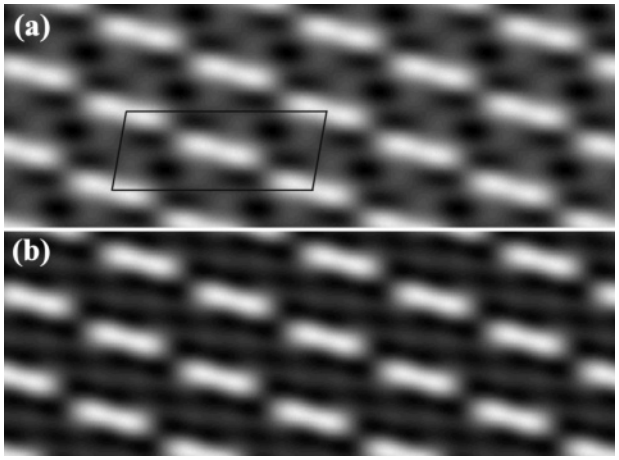

Figure 4. (a) Experimental and (b) theoretical electron density maps for the $B_{1RevTilted}$ phase of compound **1**. The crystallographic unit cell is indicated.

phases are 0. The experimental peak intensities (I_{exp}) for the B_{1Rev} phase are given in Table 2, together with the model peak intensities (I_{th}) and the corresponding form factor phases (ϕ).

The experimental and model electron density maps are shown in Figure 3. It should be noted that for the phase with a rectangular unit cell, an acceptable peak intensities ratio could also be obtained if the motif is rotated with respect to the unit-cell sides. However, the rotation of the motif would lead to partial lamellarization of the structure, resulting in the formation of the energetically costly boundaries between blocks. To exclude such a possibility, the X-ray diffraction has to be performed on a monodomain sample. For the structure with a nonrotated motif, the intensities of (hk) and ($-hk$) signals are expected to be equal. Experimentally, only very few such studies were performed and a symmetric X-ray pattern for (hk) and ($-hk$) signals was observed.[11]

The rules defining the form factors signs in the $B_{1RevTilted}$ phase are not as straightforward as in B_{1Rev}, because the possible phases of the form factors depend also on the angles δ_0 and φ. Because the molecular conformation most probably does not change significantly at phase transition from B_{1Rev} to $B_{1RevTilted}$, it can be assumed that ratio b_0/b is approximately the same in both phases and taken as $b_0 = 0.30b$. The parameter a_0 in $B_{1RevTilted}$ is at least as large as that in B_{1Rev} (where $a_0 = 0.30a$); noting that a is smaller in $B_{1RevTilted}$ we get $a_0 > 0.34a$. The δ_0 angle of the motif gives the tilt ϑ of the molecules with respect to the layer normal, thus there are two possibilities for δ_0:

$$\delta_0 - \pi/2 = \vartheta \qquad \text{and} \qquad \pi/2 - \delta_0 = \vartheta$$

The molecular tilt angle ($\vartheta \approx 10°$) was deduced from the optical measurements. Finally it should be noticed that no significant asymmetry in intensity of (11) and (−11) peaks appears unless the motif is rotated with respect to the unit cell-sides. The blocks that have the exact symmetry of the unit cell and are oriented along the unit-cell sides (ideal $B_{1RevTilted}$ structure, Figure 2b) give the same intensity of (hk) and ($-hk$) peaks in the X-ray pattern. A slight asymmetry between the signals appears if the shape of the motif is not compatible with the shape of the crystallographic unit cell. For example, if the oblique unit cell is filled with rectangular blocks, the resulting ratio of the (11) and (−11) peak intensities is 1:0.95. Thus, the only possibility for making the intensities of the (hk) and ($-hk$) peaks appreciably different is to rotate the motif against the unit-cell sides.

Within the above limits of parameter values, it is found that the signs of form factors for signals (20), (11), (−11), (−31), (02), (22), (−22), (33), and (40) are uniquely determined. The phases related to signals (−31), (−22), and (40) are π, the others have phase 0 (see Table 3). The phases of the peaks (31), (33), and (44) can be either 0 or π, depending on the magnitudes of a_0 and φ. The phase of (31) is π if $a_0 < 0.37a$, otherwise it is 0. There is no simple rule for the form factor signs of peaks (33) and (44), but their intensity is low, so that they do not affect significantly the electron density map regardless the phase. Taking the two possible phases for the form factors of peak (31), we obtain two possible experimental maps that qualitatively agree with model maps. If the phase of (31) is π, then blocks are rotated along the short diagonal, if it is 0, then they are rotated toward the short diagonal. The agreement between the model and experimental maps is better for the latter case (Figure 4). The blocks, slightly larger than in the orthogonal phase, are rotated by $\varphi \approx 10°$. The rotation angle φ is close to the molecular tilt angle, deduced from the optical measurements, and corresponds to the inclination angle of the unit cell, $\pi/2 - \delta$. The block rotation gives rise to partial lamellarization of the structure, i.e., the relative shift of the neighboring blocks is smaller than $b/2$. The actual shift between the blocks seems to be defined by the competition between two effects. Tilting of the blocks decreases the vertical shift between the neighboring blocks along the (11) direction and thus increases van der Waals interactions between the mesogenic cores of molecules, whereas making the unit cell oblique increases this shift and thus improves packing conditions of the molecular branches at the block edges. It should also be mentioned that structures of 2D modulated tilted phases are

(11) Weissflog, W.; Naumann, G.; Kosata, B.; Schroder, M. W.; Eremin, A.; Diele, S.; Vakhovskaya, Z.; Kresse, H.; Friedemann, R.; Rama Krishnan, S. A.; Pelzl, G. *J. Mater. Chem.* **2005**, *15*, 4328.

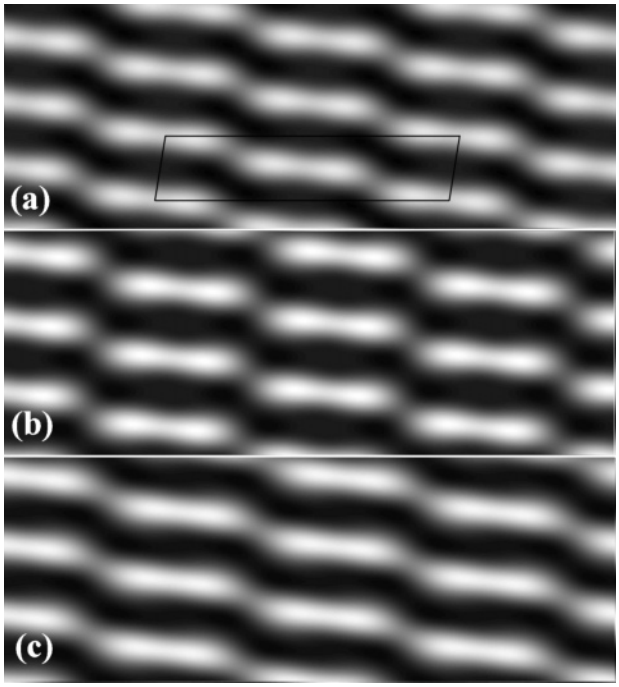

Figure 5. Experimental (a) and theoretical (b, c) electron density maps for the tilted phase of the compound **2**. Map b was obtained according to the model presented in Figure 2a, whereas map c was obtained according to the model presented in Figure 2d.

known, in which the (11) and (−11) signals are of the same intensity.[11,12] Such X-ray pattern corresponds to the ideal structure of the $B_{1RevTilted}$ phase, with the blocks arranged along the crystallographic unit-cell sides as shown in Figure 2b.

Finally, we discuss the $B_{1RevTilted}$ phase in compound **2.** In this case, the unit cell is much longer than in compound **1**. Searching for the form factor phases by putting the physically reasonable values of a_0, b_0, φ, and δ_0 in the model, we find that the form factors of the signals (20), (11), (−11) are positive, whereas form factors related to signals (40) and (−31) are always negative. The form factor (31) is positive if the rotation angle $\varphi \approx 10°$, but in that case, the experimental and model maps do not agree (the rotation of the blocks on the experimental map is close to 5°). If the form factor for signal (31) is taken to be negative, there is qualitative agreement between the experimental and the model maps (see images a and b of Figure 5). However, because the obtained experimental map suggests that there is a connection between the main blocks, we have tried to obtain better agreement in maps by assuming the anticlinic block structure with the main blocks of high electron density connected by the smaller, intermediate blocks, along the short diagonal. A model with asymmetric ripple phase was considered (Figure 2d), which improved the compatibility between the experimental and theoretical maps for compound **2** (Figure 5c).

The results obtained for the compounds **1** and **2** show that the polarization deformation, which has to appear between the blocks of opposite polarization, can be realized in two possible ways. The regions of uniform polarization can be connected either through the walls, as in material **1,** or continuously by the less ordered layer fragments, as in material **2**. It is possible that the main factor determining the type of polarization deformation between the blocks is the size of the crystallographic unit cell. For material **2**, the unit cell is considerably larger, which seems to favor continuous change of electric polarization sign through the connecting slabs. Possibly, in the connecting blocks, molecules are less tilted from the layer normal[2] than in the main blocks. Smaller tilt angle should allow for easier molecular rotation around the long molecular axis that is necessary to connect regions of opposite polarization and chirality.[3]

To conclude, we have analyzed 2D structures of the columnar phases formed by bent-core mesogenes. A theoretical model was constructed to account for the experimental X-ray diffraction data. The key procedure used in the paper is that the experimental density maps were not obtained by testing all the possible maps given by the 2^n combinations of the form factor signs, where n is the number of the experimentally obtained X-ray signals. Instead, the form factor phases were obtained from the structure model and were used in combination with the experimental X-ray signal intensities. There is a satisfactory agreement between resulting experimental and theoretical maps, so it can be concluded that the model is close to reality. The obtained maps show that in the tilted columnar phases the shift in the position of the neighboring molecular blocks is smaller that half of molecular length, whereas in the B_{1Rev} phase, it was assumed to equal half the molecular length. The blocks are connected either through the walls or continuously by the less-ordered layer fragments. The type of connection between the blocks seems to be determined by the size of the crystallographic unit cell, continuous connection being the property of the larger crystallographic unit cells.

Acknowledgment. The work was supported by the bilateral Polish-Slovenian project and Program P1-0055 financed by the MVZT, Slovenia. X-ray diffraction measurements were completed at the Structural Research Lab, Chemistry Department, Warsaw University, Poland. The Structural Research Lab has been established with financial support from European Regional Development Found in the Sectoral Operational Programme "Improvement of the Competitiveness of Enterprises, years 2004-2006", Project WKP_ 1/1.4.3./1/2004/72/72/165/2005/U.

CM0625575